An Extended Kalman Filter for frequent local and infrequent global sensor data fusion

Stergios I. Roumeliotis[1] and George A. Bekey[2]

[1]Department of Electrical Engineering
[2]Department of Computer Science
Institute for Robotics and Intelligent Systems
University of Southern California
Los Angeles, CA 90089-0781

ABSTRACT

In this paper we compare the performance of a dead-reckoning system for robot navigation to a system using an Extended Kalman Filter (EKF). Dead-reckoning systems are able to approximate position and orientation by feeding data (provided usually by local sensors) to the kinematic model of the vehicle. These systems are subject to many different sources of error. EKFs have the ability to combine the same information and compensate for most of these errors to yield a better estimate. Our simulation results using a simplified kinematic model of Rocky 7 (an experimental rover used in the Mars exploration program at Jet Propulsion Laboratory (JPL)) show that an improvement in performance up to 40% (position error) can be achieved. The local sensors used are: wheel encoders, steering angle potentiometer and gyroscope. Involvement of global sensor measurements can drastically increase the accuracy of the estimate. The lack of GPS or magnetic field on Mars narrows our choices for global localization. Landmarks, such as the sun can be used as natural beacons (reference point for absolute measurements). A sun sensor (SS) that measures the absolute orientation of the rover has been built by Lockheed Martin and now is part of the sensor suite of Rocky 7. The SS measurement is crucial for the estimation filter and we show that the accuracy of the estimation decreases exponentially as the frequency of the SS data fed to the EKF decreases.

Keywords: robot localization, sun sensor, Extended Kalman Filter

1. INTRODUCTION

In December 1996 NASA launched the pathfinder mission to Mars. On July 4th 1997, the mission deployed an autonomous micro-rover on the surface of Mars. The robot's primary mission is to do spectroscopic analysis on Martian rocks of interest to scientists on Earth. Due to challenges such as round trip communication delay time the robot is equipped to perform a high degree of autonomous goal seeking and hazard avoidance behavior.
The future missions to Mars demand longer traverses of the rover to sites of scientific interest separated by kilometers of distance (Hayati, Volpe & et al. 1996). In order to autonomously navigate and perform its scientific tasks, the rover needs to know its exact position and orientation; to localize itself.
Localization is a problem concerning every autonomous vehicle. Different kind of techniques have been developed to tackle this problem and these can be sorted into two main categories:

Relative (local) localization which consists of evaluating the position and the orientation through integration of information provided by diverse sensors. The integration is started from the initial position and is continuously updated in time.

Absolute (global) localization which is the technique that permits the vehicle to find its way directly in the domain of evolution of the mobile system. These methods usually rely on navigation beacons, active or passive landmarks, map matching or satellite-based signals like Global Positioning System (GPS).

Other author information: Email: stergios/bekey@robotics.usc.edu ; Telephone: (213) 740-7288; Fax: (213) 740-7512; URL: http://www.usc.edu/dept/robotics/; This work is supported by Jet Propulsion Labs, California Institute of Technology under contract #959816.

Local localization is also known as dead-reckoning (DR). In DR we have two basic approaches: odometric systems and inertial navigation systems (INS). In most mobile robots odometry is implemented by means of optical encoders that monitor the wheel revolutions and steering angles of the robot wheels. Using simple geometric equations (kinematic model of the vehicle), the encoder data are then used to compute the momentary position of the vehicle relative to a known starting position. INS are widely used in aviation and lately in outdoor robots. Most of them consist of gyroscopes and accelerometers that provide angular rate and velocity rate information. By integrating this rate information INS systems calculate the position and orientation of the vehicle.
Though its simplicity has made DR a widely used technique, we can not rely on it for long distances. The basic drawbacks are:

- The kinematic model of the vehicle is never accurate (for example, we do not know with infinite precision the distance between the wheel axes of the vehicle).
- The sensor models also suffer from inaccuracies and can become very complicated (for example use of exponential model for the gyroscope drift).
- The sensor readings are corrupted by noise.
- The motion of the vehicle involves external sources of error that are not observable by the sensors used (for example, slippage in the direction of motion or in the perpendicular direction).

Due to the above reasons, there is error in the calculation of the vehicle's position and orientation which generally grows unbounded with time. Substantial improvement is provided by applying Kalman filtering techniques. These techniques have been used successfully in position estimation problems such as missile tracking and ship navigation for the last four decades (Grewal & Andrews 1993) and their field of application has been extended to mobile robots. The next step to limit the error brings up the demand for absolute localization techniques. Involvement of global sensor measurements can drastically increase the accuracy of the estimate and keep the associated uncertainty within certain bounds.
In Section 2 we present examples of research relevant to the area of mobile robot localization. Section 3 contains the formulation of our problem at hand. In section 4 we compare our EKF system for localization to the simple DR using the same sensor information. Section 5 presents the impact of the frequency of the SS information to the system performance. Section 6 includes the conclusions from this research work and finally in section 7 we list the directions of our future work.

2. PREVIOUS WORK

There is considerable ongoing research effort in robot localization. In the following review we present examples of different aspects of this research.
In order to deal with systematic errors which are particulary notable in indoor applications, J. Borenstein and L. Feng present in (Borenstein & Feng 1995) a calibration technique called the UMBmark test. The dominant systematic error sources are identified as the difference in wheel diameter and the uncertainty about the effective wheel base. Thus by measuring the individual contribution of these dominant error sources (that are vehicle specific) they counteract their effect in software.
In another paper (Borenstein & Feng 1996) the same authors use measurements from odometric sensors (wheel encoders) and INS (gyroscope) during different time intervals. Their method, gyrodometry, uses odometry data most of the time, while substituting gyro data only during brief instances (e.g. when the vehicle goes over a bump) during which gyro and odometry data differ drastically. This way the system is kept largely free of the drift associated with the gyroscope and compensates for the non-systematic errors introduced by odometry.
In (Fuke & Krotkov 1996) Y. Fuke and E. Krotkov use a complementary Kalman filter introduced in (Cooper & Durant-Whyte 1994) to estimate the vehicle's attitude from the accelerometer signal in low frequency motion and the gyro signal in high frequency motion. The attitude information is then used to calculate the rotational transformation matrix from the vehicle coordinate system to the ground coordinate system. This matrix transforms the velocity information to a position increment.
In (Barshan & Durrant-Whyte 1995) the authors make best use of a low cost INS system (3 gyroscopes, a triaxial

accelerometer and 2 tilt sensors). Their approach is to incorporate in the system a priori information about the error characteristics of the inertial sensors and to use this directly in an Extended Kalman Filter (EKF) to estimate position before supplementing the INS with absolute sensing mechanisms.
On the other hand, work related to absolute localization is presented by J. J. Leonard and H. F. Durrant-Whyte. In (Leonard & Durrant-Whyte 1991) they develop a system in which the basic localization algorithm is formalized as a vehicle-tracking problem, employing an EKF to match beacon observations (environment features) to a navigation map to maintain an estimate of the mobile robot.
In (Bonnifait & Garcia 1996) the authors also use an EKF in order to fuse odometry and angular measurements of known landmarks (light sources detected using a CCD camera).
In (Baumgartner & Skaar 1994) E. T. Baumgartner and S. B. Skaar estimate a vehicle's position and orientation based on the observation of visual cues located at discrete positions within structured environment. An EKF is used to combine these visual observations with sensed wheel rotations in order to produce continuously optimal estimates.
In our work we fuse, in the same EKF structure, sensory information from odometric, INS sensors (local) with information from the SS (global). We compare the performance of our approach to the DR which has the same sensory information. In order to deal with the different rates of sensory information we apply sequential processing to the incoming measurements and we investigate the effect of the frequency of the input from the SS on the accuracy of the system.

3. FORMULATION OF THE PROBLEM

In our case the task at hand is to localize Rocky 7. We try to exploit techniques that will allow longer traverse times until the rover's position and orientation have to be determined from an external source. Instead of simple DR we apply EKF techniques that make use of the same (noisy) sensory information and combine it with the (imprecise) kinematic model in a feedback fashion such that they compensate for many of the errors previously mentioned.
A basic assumption used is that the vehicle moves on a plane. The quantities of interest are the first two moments (mean and variance) of the x, y position and ϕ, the orientation of the rover. Finally we assume that this vehicle is moving at a constant speed and steering angle in every part of its trajectory. When it wants to change its heading, it stops and does so.

3.1. Kinematic model

The kinematic model used is that of a three wheeled planar vehicle which has the steering at the rear wheel (like a fork lift).
The equations describing the kinematic model in the discrete time domain are:

$$x_{k+1} = x_k - V\Delta T \sin(\phi_k + \theta) \tag{1}$$

$$y_{k+1} = y_k + V\Delta T \cos(\phi_k + \theta) \tag{2}$$

$$\phi_{k+1} = \phi_k - \frac{V\Delta T}{b} \tan\theta \tag{3}$$

where (x_{k+1}, y_{k+1}) and (x_k, y_k): current and previous position in global coordinates,
ϕ_{k+1} and ϕ_k: current and previous orientation, V: velocity, ΔT: time increment,θ: steering angle, b: distance between the wheel axes.
Figure 1 shows the various quantities and the associated reference frames.

3.2. Sensors

The measurements are provided by:

- two encoders mounted on the two front wheels which measure the velocity of each of them.
- a potentiometer mounted on the rear wheel which provides its steering angle.

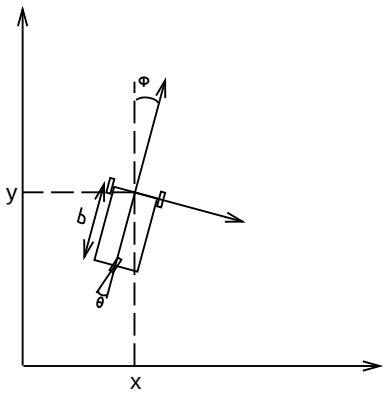

Figure 1. Planar model of the vehicle

- a gyroscope which gives the angular velocity of the vehicle on the axis perpendicular to the plane of motion.
- a sun sensor which gives the 'absolute' orientation of the vehicle according to the sun position.

The sensory measurements are corrupted by additive Gaussian noise (for most of the simulations performed the standard deviation of the noise is at least 10% of the real value of the quantity measured).
We have constructed different versions of the EKF taking into consideration terms of higher order and thus enhancing the state vector. We have compared one of the latest implementations (without the SS measurement) to the DR technique using the same sensory information. Finally we studied the performance of the EKF when the SS information is provided at varying frequencies.

4. EKF IMPLEMENTATION AND COMPARISON WITH DEAD-RECKONING

The kinematic model of the vehicle is non-linear, hence we use the Extended Kalman Filter.

4.1. Discrete Extended Kalman Filter

The EKF uses the system (kinematic) model and the measurement model. The system model describes how the vehicle's state $\mathbf{x}(k)$ changes with time in the presence of noise $\mathbf{v}(k)$:

$$\mathbf{x}(k+1) = \mathbf{f}(\mathbf{x}(k)) + \mathbf{v}(k), \tag{4}$$

where $\mathbf{f}$ is the non-linear transition function and $\mathbf{v}(k) \sim N(\mathbf{0}, \mathbf{Q}(k))$. The noise, as we have already mentioned, is assumed to be white, zero-mean Gaussian with variance $\mathbf{Q}(k)$.

The measurement model relates the sensor observations to the state of the system and has the following form:

$$\mathbf{z}(k) = \mathbf{h}(\mathbf{x}(k)) + \mathbf{w}(k), \tag{5}$$

where $\mathbf{h}$ is a non-linear function and $\mathbf{w}(k) \sim N(\mathbf{0}, \mathbf{R}(k))$. We assume that the measurements are corrupted by additive, white, zero-mean Gaussian noise with variance $\mathbf{R}(k)$.

The estimation algorithm produces an estimate of the state $\hat{\mathbf{x}}(k+1, k+1)$ of the system at time step $k+1$ based on the previously updated estimate of the state $\hat{\mathbf{x}}(k, k)$ and the observations $\mathbf{z}(k+1)$. The basic steps of the algorithm are: prediction, measurement and estimation update. We state the Kalman filter equations without derivation and we refer to (Maybeck 1982) for proofs and details.

4.1.1. Prediction

We predict the new state $\hat{\mathbf{x}}(k+1,k)$ of the system using the system model at time step $k+1$:

$$\hat{\mathbf{x}}(k+1,k) = \mathbf{f}(\hat{\mathbf{x}}(k,k)). \tag{6}$$

and the covariance $\mathbf{P}(k+1,k)$ associated with this prediction:

$$\mathbf{P}(k+1,k) = \mathbf{F}(k)\mathbf{P}(k,k)\mathbf{F}^T(k) + \mathbf{Q}(k), \tag{7}$$

where $\mathbf{F}(k)$ is the Jacobian of $\mathbf{f}$ obtained by linearizing about the updated state estimate $\hat{\mathbf{x}}(k,k)$:

$$\mathbf{F}(k) = \nabla\mathbf{f}(\hat{\mathbf{x}}(k,k)). \tag{8}$$

Finally we compute the predicted measurements using the updated state estimate $\hat{\mathbf{x}}(k,k)$:

$$\hat{\mathbf{z}}(k+1) = \mathbf{h}(\hat{\mathbf{x}}(k+1,k)). \tag{9}$$

4.1.2. Measurements

In this step we get the actual measurements $\mathbf{z}(k+1)$ and we compare them to the predicted ones $\hat{\mathbf{z}}(k+1)$. The difference between them is the measurement residual (or innovation):

$$\mathbf{r}(k+1) = \mathbf{z}(k+1) - \hat{\mathbf{z}}(k+1). \tag{10}$$

At this point we calculate the covariance of the residual:

$$\mathbf{S}(k+1) = \mathbf{H}(k+1)\mathbf{P}(k+1,k)\mathbf{H}^T(k+1) + \mathbf{R}(k+1), \tag{11}$$

where $\mathbf{H}(k+1)$ is the Jacobian of $\mathbf{h}$ obtained by linearizing about the state estimate $\hat{\mathbf{x}}(k+1,k)$:

$$\mathbf{H}(k+1) = \nabla\mathbf{h}(\hat{\mathbf{x}}(k+1,k)). \tag{12}$$

4.1.3. Estimation update

In the last step of the estimation algorithm we use the measurement residual $\mathbf{r}(k+1)$ to correct the state prediction $\hat{\mathbf{x}}(k+1,k)$ and thus compute the updated state estimate $\hat{\mathbf{x}}(k+1,k+1)$. In order to do that we calculate the Kalman gain:

$$\mathbf{W}(k+1) = \mathbf{P}(k+1,k)\mathbf{H}^T(k+1)\mathbf{S}^{-1}(k+1), \tag{13}$$

and then we update the state prediction:

$$\hat{\mathbf{x}}(k+1,k+1) = \hat{\mathbf{x}}(k+1,k) + \mathbf{W}(k+1)\mathbf{r}(k+1). \tag{14}$$

Finally we compute the associated covariance:

$$\mathbf{P}(k+1,k+1) = \mathbf{P}(k+1,k) - \mathbf{W}(k+1)\mathbf{S}(k+1)\mathbf{W}^T(k+1). \tag{15}$$

This will be used as the new state covariance in the next iteration of the estimation algorithm.

4.2. System and measurement vectors

4.2.1. System Vector

In our earliest implementations of the EKF the system state was composed of x, y, ϕ, $V$and θ (estimated position, orientation, velocity and steering angle). The basic drawback of these implementations, derived from simulation experiments, was that they were not very sensitive to changes in the vehicle's orientation caused by external sources of noise like slippage. **The error in the orientation is the most crucial one because it causes constant growth of the position error right after it occurs.** Motivated from this observation we enhanced the state vector $\mathbf{x}$ with the angular velocity, $\dot{\phi}$ and the angular acceleration $\ddot{\phi}$.
Next, seeking better results in the velocity tracking of the vehicle, we augmented the state vector introducing $\dot{V}$, the acceleration of the vehicle, as an additional state variable in the filter. This new state variable increases the order of the system and by doing so allows the enhanced filter to track faster changes in the velocity of the rover.

Thus the vector that we use to describe the state of the system is $\mathbf{x} = [x, y, \phi, \dot{\phi}, \ddot{\phi}, V, \dot{V}, \theta]^T$.

4.2.2. Measurement Vector

The measurement vector is composed by the measured quantities: V_1, V_2 (velocities of the wheels provided by the wheel encoders), $\dot{\phi}$ (angular velocity provided by the gyro) and θ (the steering angle provided by the potentiometer). The steering angle measurement is redundant since it is also calculated using the velocity observations V_1 and V_2 as:
$\theta = \tan^{-1}(\frac{V_2 - V_1}{V}\frac{b}{a})$, where a is the width of the vehicle. The vector that contains the available measurements is $\mathbf{z} = [V_1, V_2, \dot{\phi}, \theta]^T$.

4.3. Dead-Reckoning

The DR technique uses the kinematic model of the system which is fed with the measured quantities and calculates the change in the position and the orientation of the vehicle. Computationally it is simpler than the EKF but the associated uncertainty grows faster than in the EKF case.
In order to have a better insight into the superiority of the EKF technique, which takes into account both the system and the sensor models, over the simple DR technique we cite the following figures:
In figure 2 an example of a trajectory is presented (the distance covered is 18m); in Figure 3 we show the average absolute error in position over 10 trials for different steering angles that cause trajectories that vary from straight line to half-circle.
For these simulation experiments the sensor noise levels were (standard deviations): $\sigma_{V_1} = 2cm/sec, \sigma_{V_2} = 2cm/sec, \sigma_{\dot{\phi}} = 0.0031rad/sec$ (each of them is 20% of their nominal value) and $\sigma_\theta = 0.31rad (= 20\%\pi/2)$.
The sensor data were available at 50Hz and the velocity of the vehicle was 10 cm/sec

5. SUN SENSOR INFLUENCE ON THE SYSTEM PERFORMANCE

In order to bound the uncertainty in our estimation we need global measurements that will update some of the states of interest x, y or ϕ and so eliminate the accumulated error. The lack of a strong magnetic field on Mars prohibits the use of a compass. On the other hand GPS signals are not detectable that far away and there are no accurate maps of the Martian surface to a level that would enable landmark recognition and map matching techniques.
For these reasons a sun sensor has been developed by Lockheed-Martin (Hayati, Volpe, Backes, Balaram, Welch, Ivlev, Tharp, Peters, Ohm, Petras & Laubach 1997) that provides heading information. The SS (also known as wide angle sun sensor) has a 160 degrees field-of-view and uses the additional pitch and roll information provided by an accelerometer to calculate the vehicle's orientation ϕ. The SS is already part of the sensor suite of Rocky 7 and shortly it will be tested in field trials. The fact that it is the only available source of absolute information motivates us to investigate its influence on the system performance. In the previous Section we assumed that all the measurements appear at the same frequency and we chose to apply simultaneous processing. In the case of the SS the position of the sun on the sensor's surface (x_R, y_R) is transformed to an angle through a 160x160 calibration table. The time to access this look up table limits the frequency at which the SS measurements are available. As a result of this, in our EKF system we have to deal with different rates of sensory input. We tackle this problem by applying sequential processing to these data. The two schemes (simultaneous, sequential) are equivalent. For proofs and details on that we refer the reader to (Sorenson 1966).

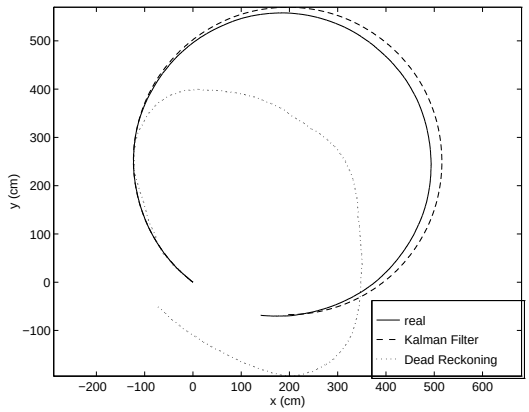

Figure 2. Comparison Extended Kalman Filter vs. Dead-Reckoning

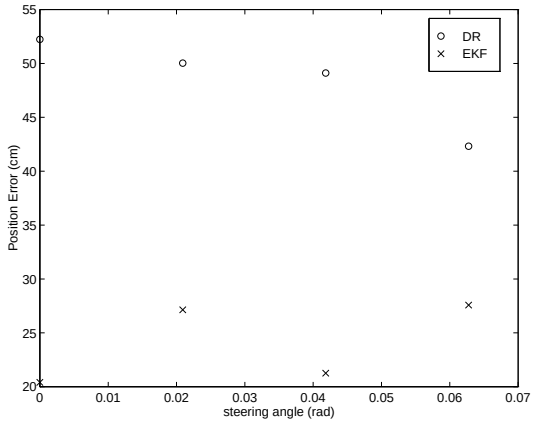

Figure 3. Comparison Extended Kalman Filter vs. Dead-Reckoning

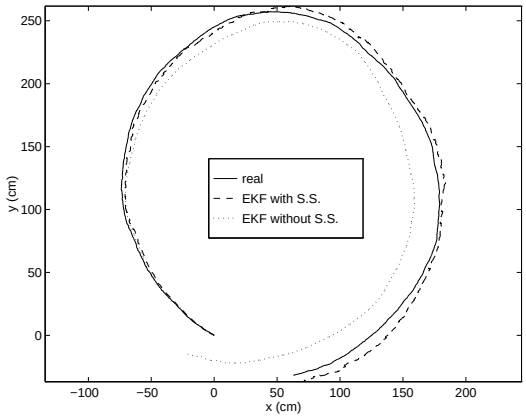

Figure 4. Trajectory estimate comparison between the the EKF with the SS and the EKF without the SS measurement. $f_{SS} : f_{othersensors} = 1 : 1$

5.1. Sequential Processing

The formulation of the EKF equations for the sequential processing case differs as follows:
In 4.1.1 the same equations are used to predict the next state of the system. In 4.1.2 instead of (10), (11), (12), we use:

$$r_i(k+1) = z_i(k+1) - \hat{z}_i(k+1), \tag{16}$$

where z_i is the measurement provided by the ith sensor only and $\hat{z}_i$ is the predicted value for that measurement.

$$S^i(k+1) = \mathbf{H}^i(k+1)\mathbf{P}^i(k+1,k)\mathbf{H}^{iT}(k+1) + R_{i,i}(k+1). \tag{17}$$

is the covariance of the residual of the latest measurement, where

$$\mathbf{H}^i(k+1) = \frac{\partial h_i(\hat{\mathbf{x}}^i(k+1,k))}{\partial \hat{\mathbf{x}}^i}. \tag{18}$$

In 4.1.3 instead of (13), (14), (15), we have:

$$\mathbf{W}^i(k+1) = \mathbf{P}^i(k+1,k)\mathbf{H}^T(k+1)/S^i(k+1), \tag{19}$$

where $\mathbf{W}^i(k+1)$ is the filter gain based on the measurement $z_i(k+1)$ only. The updated state prediction after the latest measurement is:

$$\hat{\mathbf{x}}^{i+1}(k+1,k) = \hat{\mathbf{x}}^i(k+1,k) + \mathbf{W}^i(k+1)r_i(k+1). \tag{20}$$

and the associated covariance:

$$\mathbf{P}^{i+1}(k+1,k) = \mathbf{P}^i(k+1,k) - \mathbf{W}^i(k+1)S^i(k+1)\mathbf{W}^{iT}(k+1), \tag{21}$$

The computed quantities $\hat{\mathbf{x}}^{i+1}(k+1,k), \mathbf{P}^{i+1}(k+1,k)$ will be used in (17) and (18) if there is a new measurement at this time, otherwise these will be the $\hat{\mathbf{x}}(k+1,k+1), \mathbf{P}(k+1,k+1)$ resulting from the current iteration of the estimation algorithm. The state vector is the same as before; $\mathbf{x} = [x, y, \phi, \dot{\phi}, \ddot{\phi}, V, \dot{V}, \theta]^T$.

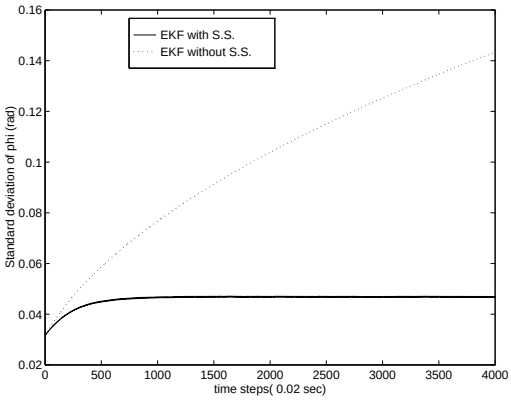

Figure 5. Standard deviation of the orientation of the vehicle (σ_ϕ) for the EKF with the SS and the EKF without the SS measurement. $f_{SS} : f_{othersensors} = 1 : 1$

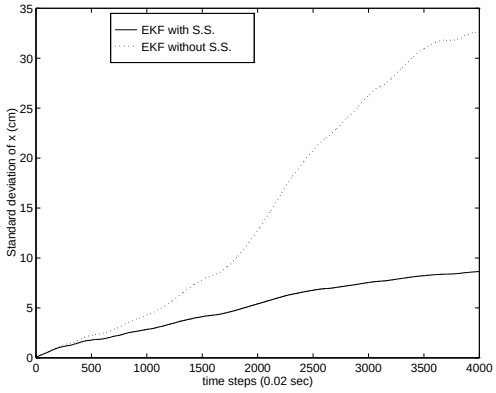

Figure 6. Standard deviation of the position of the vehicle (σ_x) for the EKF with the SS and the EKF without the SS measurement. $f_{SS} : f_{othersensors} = 1 : 1$

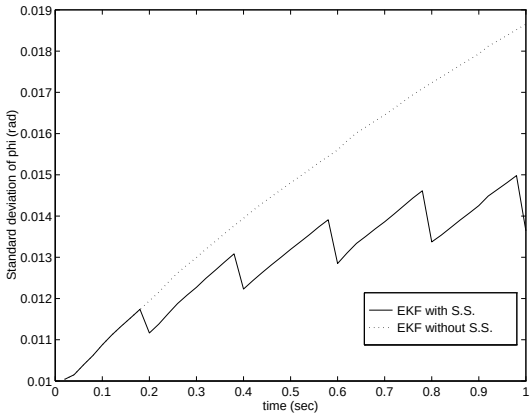

Figure 7. Standard deviation of the orientation of the vehicle (σ_ϕ) for the EKF with the SS and the EKF without the SS measurement. $f_{SS} : f_{othersensors} = 1 : 10$

The measurement vector is augmented to include the SS measurement. This is the absolute orientation ϕ of the vehicle with reference point the sun. Thus $\mathbf{z} = [V_1, V_2, \dot{\phi}, \theta]^T$.
In the simulation experiments conducted, the noise level for the SS is: $\sigma_\phi = 0.314 rad$ (10% of π), while for the rest of the sensors it is the same as before. The previously considered sensors continue to provide measurements at 50Hz and the vehicle's velocity remains 10cm/sec.
In order to explore the influence of the SS we cite the following figures:
In figure 4 we can see the real (actual) trajectory for a particular trial in comparison to the two estimates provided by the two EKFs. The one that uses the SS measurements and the one that does not. Figure 5 shows the standard deviation of the orientation ϕ of the vehicle (σ_ϕ) for the two cases (same experiment). It is obvious that σ_ϕ is bounded when the SS is involved which means that the uncertainty for the vehicles orientation is also bounded.
Figure 6 shows the standard deviation for the vehicle's position x (σ_x) also for the same experiment. Though σ_x grows with time in the SS EKF case, the rate of growth is definitely smaller than in the non-SS EKF case where global measurements are not available. This is expected since the error in orientation has great impact on the position estimate. Similar results were observed for the standard deviation of y as well.
In the previous experiment we had the same input frequency for the SS and the rest of the sensors. In figure 7 the standard deviation of the orientation ϕ of the vehicle (σ_ϕ) is represented but now the SS provides information to the SS EKF with rate 10 times smaller compared to the rest of the sensors. The figure is purposely limited to the first 50 steps of the estimation algorithm in order to make observable the instant decrease of the orientation uncertainty each time a new absolute measurement is provided to the SS EKF (this happens at t = 0.2, 0.4, 0.6, 0.8, 1.0 seconds). The orientation uncertainty in this case is increasing but the rate is lower than in the non-SS EKF case.
In order to evaluate the influence of the frequency of the SS measurements on the performance of the EKF we conducted the following simulation experiments: 10m traverses for different sensor frequencies ratios. $f_{othersensors}/f_{SS}$ varied from 1 to 10. 20 different trials were performed and the average (absolute) error in position and orientation is shown in figures 8 and 9. In the same figures the position and orientation accuracy are shown as percentages. The accuracy characterizes the performance of the system and as we can see it decreases exponentially as the SS measurements become more and more infrequent.

6. CONCLUSIONS

One of the conclusions derived from this work is that the EKF provides the rover with position and orientation estimates superior to these calculated by DR. It was also shown that the inclusion of a global sensor, which was the SS, had considerable affect on the uncertainty of the estimates. Finally the impact of the frequency of the SS measurements on the system performance was shown. This last conclusion shows that it is of great importance to

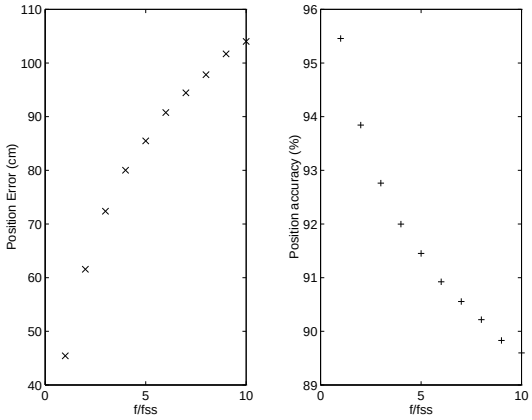

Figure 8. Position error and accuracy for different frequencies of the SS measurements

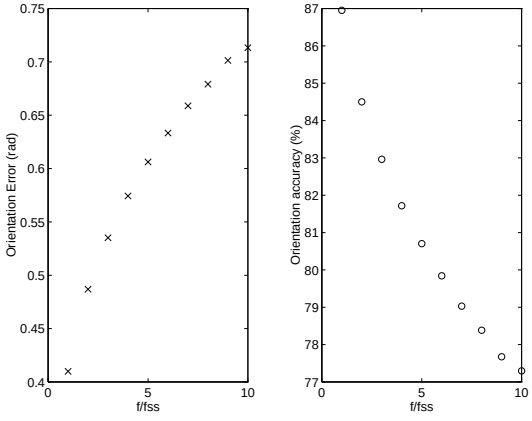

Figure 9. Orientation error and accuracy for different frequencies of the SS measurements

have the SS measurements flowing into the EKF at frequency as high as the frequency of measurement flow from the other sensors. Currently the $f_{SS} = \frac{1}{5} f_{othersensors}$.

7. FUTURE WORK

This paper presents first results from the ongoing research effort related to the localization of Rocky 7. Within our goals in the near future is to define and use a more accurate kinematic model of the rover that will enable us to expand the estimation to the 3D space. We also plan to fuse extra information from sensors not used in the current implementation (such as the accelerometers). Finally we expect to use data from the real rover to tune the EKF appropriately.

ACKNOWLEDGEMENTS

The authors would like to thank S. Hayati, G. Rodriguez, R. Volpe for insightful discussions over the past few months and E. Baumgartner for useful comments. The authors also thank G. Sukhatme for his constant support and precious contribution to this research effort.

REFERENCES

Barshan, B. & Durrant-Whyte, H. F. (1995), 'Inertial navigation systems for mobile robots', *IEEE Transactions on Robotics and Automation*.

Baumgartner, E. T. & Skaar, S. B. (1994), 'An autonomous vision-based mobile robot', *IEEE Transactions on Automatic Control*.

Bonnifait, P. & Garcia, G. (1996), A multisensor localization algorithm for mobile robots and it's real-time experimental validation, *in* 'Proceedings of the 1996 IEEE International Conference on Robotics and Automation'.

Borenstein, J. & Feng, L. (1995), Correction of systematic odometry errors in mobile robots, *in* 'Proceedings of the 1995 IEEE International Conference on Robotics and Automation'.

Borenstein, J. & Feng, L. (1996), Gyrodometry: A new method for combining data from gyros and odometry in mobile robots, *in* 'Proceedings of the 1996 IEEE International Conference on Robotics and Automation'.

Cooper, S. & Durant-Whyte, H. F. (1994), A frequency response method for multi-sensor high-speed navigation systems, *in* 'In Proceedings of IEEE Conference on Multisensor Fusion and Integration Systems'.

Fuke, Y. & Krotkov, E. (1996), Dead reckoning for a lunar rover on uneven terrain, *in* 'Proceedings of the 1996 IEEE International Conference on Robotics and Automation'.

Grewal, M. S. & Andrews, A. P. (1993), *Kalman Filtering, Theory and Practice*, Prentice Hall.

Hayati, S., Volpe, R. & et al. (1996), Microrover research for exploration of mars, *in* 'Proceedings of the 1996 AIAA Forum on Advanced Developments in Space Robotics', University of Wisconsin, Madison.

Hayati, S., Volpe, R., Backes, P., Balaram, J., Welch, R., Ivlev, R., Tharp, G., Peters, S., Ohm, T., Petras, R. & Laubach, S. (1997), The rocky 7 rover: A mars scientific prototype, *in* 'Proceedings of the IEEE International Conference on Robotics and Automation', Albaquerque, NM.

Leonard, J. J. & Durrant-Whyte, H. F. (1991), 'Mobile robot localization by tracking geometric beacons', *IEEE Transactions on Robotics and Automation*.

Maybeck, P. S. (1982), *Stochastic Models, Estimation and Control*, Academic Press.

Sorenson, H. W. (1966), *Advances in Control Systems*, Vol. 3, Academic Press, chapter Kalman Filtering Techniques.